Tech Brief: Axial Fan Research for Automotive and Building Ventilation Applications

John F. Foss[1], Scott C. Morris[2], Douglas R. Neal[2]

[1]Professor, Department of Mechanical Engineering, Michigan State University
[2]Graduate Research Assistant, Department of Mechanical Engineering

INTRODUCTION

Axial fans provide airflows over an extremely large range of flow rates and pressure rise values. Their distinguishing feature is that the pressure rise will be relatively small and the flow rate relatively large in comparison with prime movers of other designs, e.g., cent-axial and centrifugal. Numerous general discussions of axial fans exist; the following are among those that can be recommended: Wallis (1961), Osborne (1966), and Bleier (1998).

The present communication is to provide a focus on two classes of fans that have been investigated in the writers' laboratory. These two classes can be described in terms of the application areas served: automotive engine thermal management and agricultural building ventilation. The importance of the former is apparent when one realizes that nominally one-third of the released energy in the combustion process must be transferred to the ambient air through the cooling water jacket and the radiator. (Air conditioning and auxiliary heat exchangers add to this thermal "load".)

Numerous factors make prediction of the underhood cooling flows a most challenging task. Among these are the influence of the upstream restrictions on the fan performance and the blockage elements that exist downstream of the fan. Lifting the hood on a modern passenger car will immediately clarify this issue. These complexities and the importance of properly addressing them has provided the motivation for auto manufacturers to invest in detailed investigations of these flows. As specific examples, the writers' efforts have been supported by

the Ford Motor Co. (now including Visteon, Inc.) and DaimlerChrysler; some of the results from these investigations are presented below.

Axial fans found in agricultural applications include those used in greenhouse and livestock building ventilation. Heat and moisture removal, along with the discharging of contaminated air are the primary issues for these ventilation systems. Two specific applications, poultry and swine production are described below.

Poultry buildings are typically 18 m (60 ft) wide × 122 m (400 ft) long and house 100,000 birds. In these buildings, air is exhausted via an array of axial fans located along the width of one end. Clean air is then drawn in through the opposite end, where it is either cooled via evaporative heat exchangers or conditioned through a series of filters. This system is termed "tunnel ventilation". During the summer months, heat removal is critical; it can be readily appreciated that a failure of the airflow system would cause catastrophic losses as the temperature in the building would dramatically increase with 100,000 birds serving as localized heat sources, producing 7.2 watts/bird (or 12 BTU/hour/bird). During the winter months, heat removal is less of a concern, but moisture removal and oxygen replacement become increasingly important. Egg production and weight gain (meat) are adversely affected by increased temperature and decreased amounts of fresh air. For the farmer/producer, enhanced air-moving efficiency will translate directly into increased profits given that the fans account for nominally 50-60 percent of the operation's total costs.

The size of a swine building varies depending on the stage of the animals' development (the swine are moved into different buildings as they grow). For the "finishing" stage, which is the final stage and thus houses the swine at their largest size, the building is typically 12 m (40 ft) wide × 60 m (200 ft) long and houses 1000 animals. In these facilities, heat and moisture

removal are the most critical issues in the summer; in the winter, moisture and ammonia removal (a potentially suffocating by-product from the animal's waste), along with oxygen replacement are the most important considerations. It is noted that "cleansing the discharge air" is both environmentally friendly as well as costly in terms of the additional pressure rise across (or power input to) the induction fans.

The limited profit margins in these facilities places a premium on the cost effective provision of the needed airflows. This motivation led to Phase I and Phase II USDA/SBIR contracts to Digital Flow Technologies, Inc. (DFTI) with subcontracts made available to the writers' laboratory. A leading manufacturer of such fans: Aerotech, Inc. of Mason, MI, has partnered with DFTI to commercialize these developments. The USDA and the Aerotech, Inc. support has also led to the results summarized below.

GENERAL CONSIDERATIONS REGARDING AXIAL FANS

The essential character of an axial fan is revealed by a lifting surface (an airfoil) that is translating in a quiescent medium. Following the passage of the surface, the drag experienced by the surrounding fluid will lead to an in-line component of velocity and the lift on the surface will produce a corresponding momentum flux in the direction opposite to the lift.

If the lifting surface were a fan blade, these motions could be resolved into the azimuthal and axial velocity components downstream of the fan. Since the airfoil sections experience a translation velocity of magnitude $(\vec{\Omega}\times\vec{R})$, and since the blade will not have a uniform shape for all (R), the induced velocities may be a complicated function of R. Concomitant effects, developed by the centrifugal $(-\vec{\Omega}\times\vec{\Omega}\times\vec{R})$ and the Coriollis $(-2\vec{\Omega}\times\vec{V})$ "force" effects and augmented by a pressure rise across the fan plane, will lead to a radial velocity component in the induced motion. It is useful to note that the technological motivation for an axial fan: "to move

fluid from the upstream to the downstream domains" is primarily achieved by the axial component. A positive radial component, depending upon the fan/shroud geometry, may also contribute to the mass flux. The azimuthal component simply represents an "energy sink".

The standard description of a fan's performance is given in terms of the pressure rise (ΔP) as a function of the flow rate (Q). These variables are best considered in dimensionless form. The length and velocity scales most commonly used are the fan diameter (D) and tip speed (U_{tip}), respectively. The pressure coefficient:

$$\psi=\Delta P/\rho\, U_{tip}^2 \tag{1}$$

and the flow coefficient

$$\phi=Q/(\pi D^2/4)U_{tip} \tag{2}$$

are defined to provide a new functional dependence: $\psi=\psi(\phi)$. For a given blade shape, this relationship will be valid for a wide range of fan sizes and speeds. This reflects the insensitivity of the flow field to the Reynolds number. That is, the non-dimensional velocity and pressure fields are dominantly controlled by inertial effects and the imposed boundary conditions; they are insensitive to viscous effects. The above dimensional reasoning leads to what is conventionally referred to as "fan laws". Specifically, the scaling of dependent variables which are independent of Reynolds number provides a set of standard relationships commonly found in the literature and texts.

Figure 1 shows a typical automotive cooling fan installed in a test configuration. The geometrical configuration for this test is referred to as a 'free inlet-free outlet' or FIFO condition. This configuration is used to benchmark fan performance without the effects of blockage elements. The latter, which are in close proximity to the installed fan, significantly affect its performance.

Figure 2 shows a typical building ventilation fan. This 0.67m (26.5-inch) diameter fan is typical of the fans that would be found in hog buildings. The performance is also typical in that a relatively low pressure rise and high volume flow rate are provided. Several aerodynamic differences exist between the automotive and ventilation fans which lead to these different performance characteristics. Specifically, the number of blades, hub-to-tip ratio, and solidity are design parameters which play an important role in a fan's performance and all of these are larger for the automotive fan.

A variable which is also of considerable interest is the fan efficiency. Unlike performance, the definition of efficiency depends on the specific application of the fan. For automotive cooling fans, the chosen velocity and length scales are used to normalize the input power. The definition of efficiency follows (where ρ_{shaft} is the power delivered to the fan's drive shaft):

$$\eta = \frac{\Delta PQ}{P_{shaft}} \tag{3}$$

The ventilation industry typically defines efficiency as a dimensional number: flow rate/input power. This is usually expressed in CFM/Watt.

THE AXIAL FAN RESEARCH AND DEVELOPMENT FACILITY

Figure 3 presents the performance ($\Delta p \sim Q$) and the efficiency data for the fan/shroud combination of Fig. 1. These data are presented in non-dimensional form which would permit their extension for other rpm values (1000 rpm was used for the plot) and for other geometrically similar configurations. The experimental data for Figure 3 were acquired in a unique facility: the Axial Fan Research and Development (AFRD) facility located in the Turbulent Shear Flows Laboratory at Michigan State University. This flow system in shown in Figure 5.

Laboratory air is delivered through the test-fan-plane into the upper receiver of the AFRD. The corresponding Δp is easily measured via the indicated pressure tap. A novel moment-of-momentum flux device (see Fig. 6 and Morris, et al. (2000)) is used to determine the volume flow rate delivered by the test fan against the back pressure of the upper receiver. This pressure is controlled by the throttled condition of the large centrifugal fan which exhausts the lower receiver of the AFRD. This complete system has been fully described in the MS thesis by Morris (1997). Morris and Foss (1998) provides a more readily available description. For convenience, these two references are identified as (M97) and (M/F) below.

The favorable attribute of the moment-of-momentum flux flow meter is its insensitivity to the approach flow condition. This is important given the large variations that are experienced in the AFRD. Specifically, the unobstructed flow from the fan will be downward to the floor of the upper receiver and it will horizontally enter the nozzle contraction. Conversely, an obstructed fan flow (e.g., a simulated engine which blocks the fan flow) will enter the nozzle from the outer walls of the upper receiver.

A 15 HP, ±1% speed controlled drive system is used to power the automotive cooling fans. This drive train includes a torque meter that permits an accurate (≐0.15% of full scale) measure, when combined with the fan's rotational speed of the delivered power. Independent electrical measurements allow the drive train losses to be assessed and they provide a consistency check on the direct power measurement.

Detailed hot-wire surveys can be executed in the outflow from the fan. For these, a calibrated x-array of hot-wire sensors is aligned with the time mean flow direction that has been independently determined using the technique described by M97 and M/F. A three-dimensional probe alignment device (see Fig. 7) is used to support the probe shaft with the correct spherical

angles of the time mean velocity. The time series data (E_1, E_2) then allow $u(t)$ – plus – $v(t)$ and, with a 90-degree rotation about the probe axis, $u(t)$ – plus – $w(t)$ to be acquired. These Cartesian components: u,v,w are referenced to the "probe coordinates for each measurement. The time resolved velocity data can be used to recover the time mean, the fluctuation intensities, and the kinematic Reynolds shear stress quantities in the axial, tangential directions if the probe is in this plane for the u,v measurements. (This is the condition for the data presented below). The time mean and fluctuating intensity data for the radial velocity component follow from the u,w data given the same constraint.

Figures 8 and 9, which were obtained using the configuration of the next section, are included here as demonstrations of the level of detail that can be obtained from the measurements described above. These data have been abstracted from M97 and the manuscript that has been submitted to *JFE*: Morris and Foss (2000). One quadrant of the full data set is shown. These phase sampled data are referenced to the fan's angular position (θ) by an optical encoder which is reset (n=0,1,2…N) for each revolution. The ensemble averaged data represent 900 independent samples, i.e., N=899.

Note that the signatures of the blades are well resolved in these data. The spatially differentiated $\overline{v}_r(r,\theta)$ and $\overline{v}_\theta(r,\theta)$ data permit the axial vorticity

$$\omega_x = \frac{\partial v_\theta}{\partial r} + \frac{v_\theta}{r} - \frac{1}{r}\frac{\partial v_r}{\partial \theta} \tag{4}$$

to be determined. The wingtip vortex motions are clearly evident in Fig. 9.

THE AERODYNAMIC SHROUD (AN MSU INVENTION)

The aerodynamic shroud, shown schematically in Fig. 10 and described by Foss (1998) and Foss and Morris (1999), provides two distinct benefits for the axial fans considered in this communication. An engine driven fan must be configured with a large tip clearance given the

relatively large (≈25mm) motion between the chassis mounted shroud and the engine mounted fan. A concomitant result of this condition is the presence of large "tip region losses" or flows from the pressure to the suction side of the blade in the tip region. A ventilation fan will typically operate with a small tip clearance, but the downstream diffuser cone is vulnerable to flow separation effects given the limited energy that can be supplied to the boundary layer fluid by the fan. In both of these conditions, the enhanced axial momentum at the fan plane, as provided by the Coanda jet of the aeroshroud, leads to improved system performance. A recent study by Neuendorf and Wyganski (1999) has identified the benefits of using a properly shaped inlet shroud contraction. Their identification of an enhanced entrainment for a curved surface wall jet will be investigated in our search for an improved aeroshroud design.

The beneficial influence of the aeroshroud on the automotive fan's performance is clearly shown by the $\Delta p \sim q$ curves of Fig. 11. M97 showed that the product of the aeroshroud's flow rate and pressure rise – i.e., its power – correlated the performance data. This product, suitably non-dimensionalized, is shown as the parameter X in Fig. 11. Its definition is:

$$X=\Delta PQ/\rho A_{flow} U_{tip}^{3} \tag{5}$$

Significant performance improvements were also experienced in the ventilation fan studies. The configuration, shown in Fig. 12, when fitted with an active aeroshroud, achieved the performance improvements shown in Table 1. These numerical values represent a pressure rise condition of 0.1 inches of water; however, similar gains were observed for all pressure rise conditions.

Table 1: Performance improvements for the ventilation fan that has been fitted with an aeroshroud

	Without Aeroshroud	With Aeroshroud	% Difference
Q	61.5	79.5	29.2

Efficiency	15.9	16.8	6.11

Note, the efficiency improvement was assessed using an estimated 70% efficient centrifugal fan to pressurize the aeroshroud. Also, since the inflow to the aeroshroud can be taken from the building to be ventilated, the figures in Table 1 include the shroud flow rate in the enhanced Q value.

SUMMARY

Axial fans are utilized in a wide range of applications. Two of these: underhood cooling fans and building ventilation fans have been considered in this communication. The writers' capability to execute detailed velocity measurements, as well as performance measurements, has been demonstrated. An MSU invention: the aerodynamic shroud, has been shown to enhance the performance of both styles of fans.

REFERENCES

Bleier, F.P., *Fan Handbook: selection, application, and design*, New York: McGraw-Hill c1998.

Foss, J.F., "Improved Cooling Fan Shroud," U.S. Patent No. 5,762,034, 1998.

Foss, J.F. and Morris, S.C., "Fan Shroud with Integral Air Supply," U.S. Patent No. 5,991.685, 1999.

Morris, S.C., Neal, D.R., Foss, J.F., Cloud, "A Unique Airflow Measurement Device," submitted to *Meas. Sci. Tech*. 2000.

Morris, S.C., "Experimental Investigation of an Aerodynamic Shroud for Cooling Fan Applications," Masters Thesis, Michigan State University, Dept. of Mechanical Engineering, 1997.

Morris, S.C., Good, J.J., Foss, J.F., "Velocity Measurements in the Wake of an Automotive Cooling Fan," *Experimental Thermal and Fluid Science*, vol. 17, pp100-106, 1998.

Morris, S.C., Foss, J.F., "Performance Measurements of an Aerodynamic Fan Shroud," submitted to *J. Fluids Engineering*, 2000.

Nuendorf, R. and Wyganski, I., "On a turbulent wall jet flowing over a circular cylinder", *Journal of Fluid Mechanics*, vol. 38, 1999, pp. 1-25.

Osborne, W.C., *Fans*, New York: Pergamon Press 1996.

Wallis, A.R., *Axial Flow Fans: design and practice*, New York: Academic Press 1961.

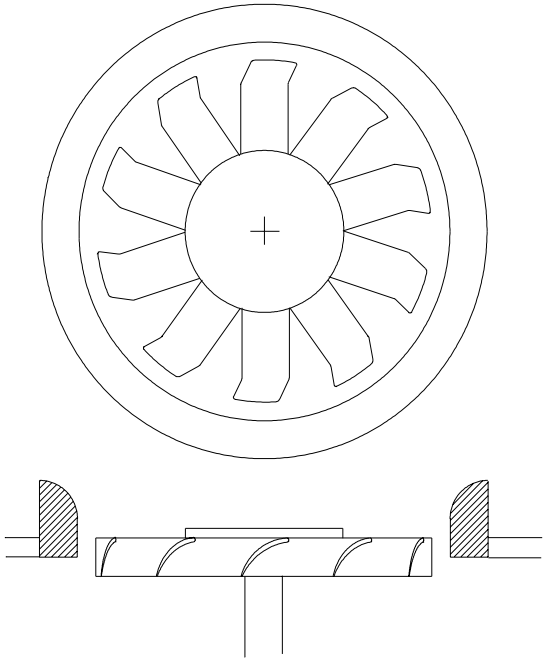

Figure 1. A typical underhood cooling fan in a shroud that permits the free inflow/free outflow (FIFO) condition to be examined.

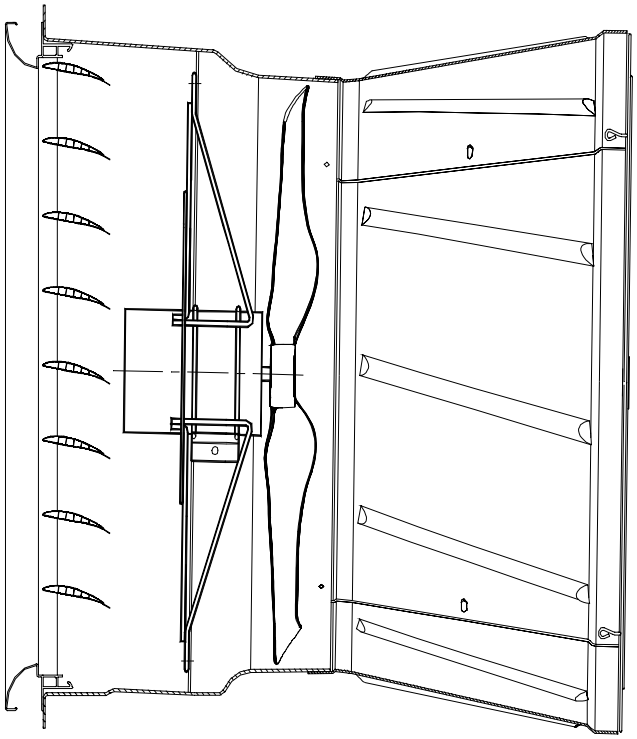

Figure 2. Aerotech 26 inch axial fan with inlet shutter and diffusor cone.

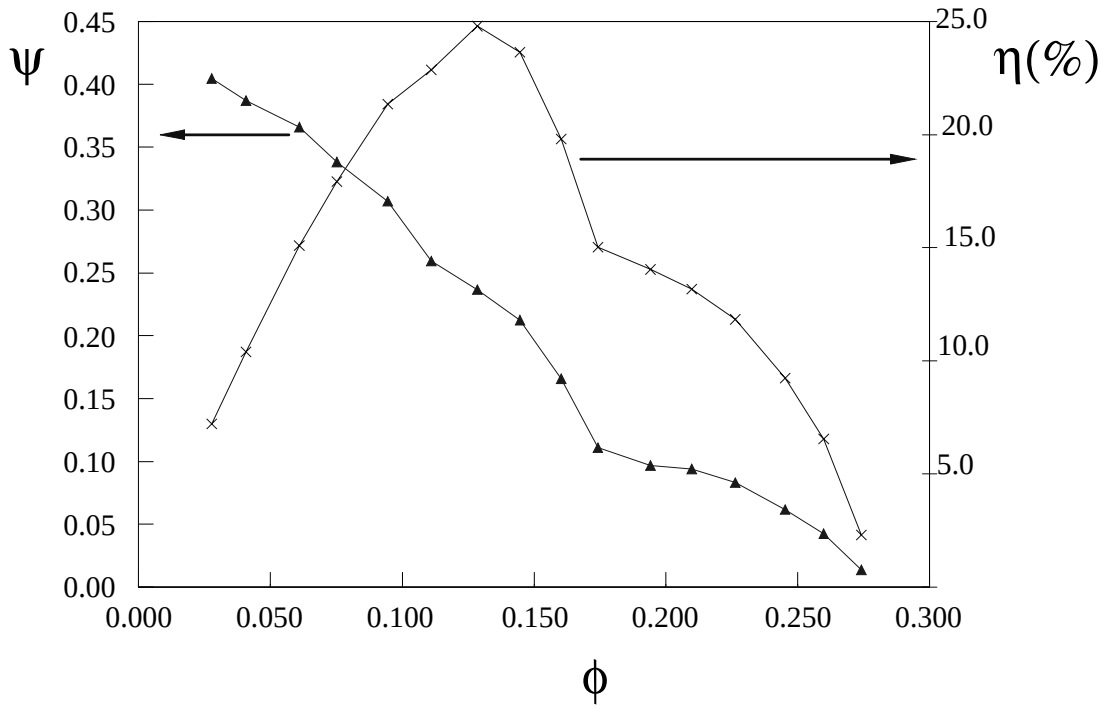

Figure 3. The nondimensional pressure rise (ψ) and efficiency (η) as a function of the nondimensional flow rate. Note, see equations 1, 2 and 3 for ψ, ϕ and η.

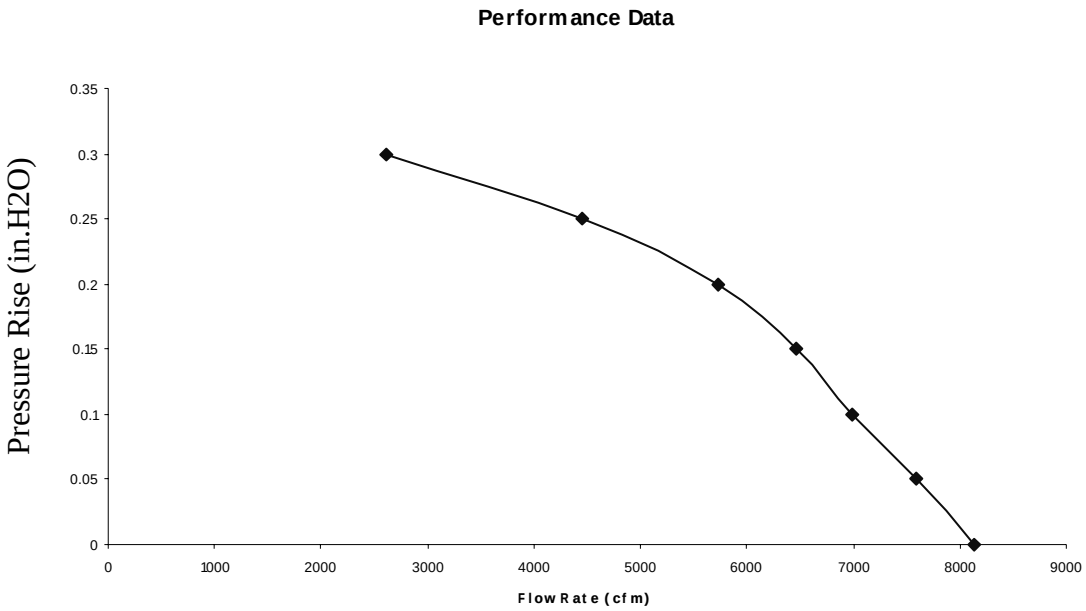

a) pressure rise as a function of the flow rate

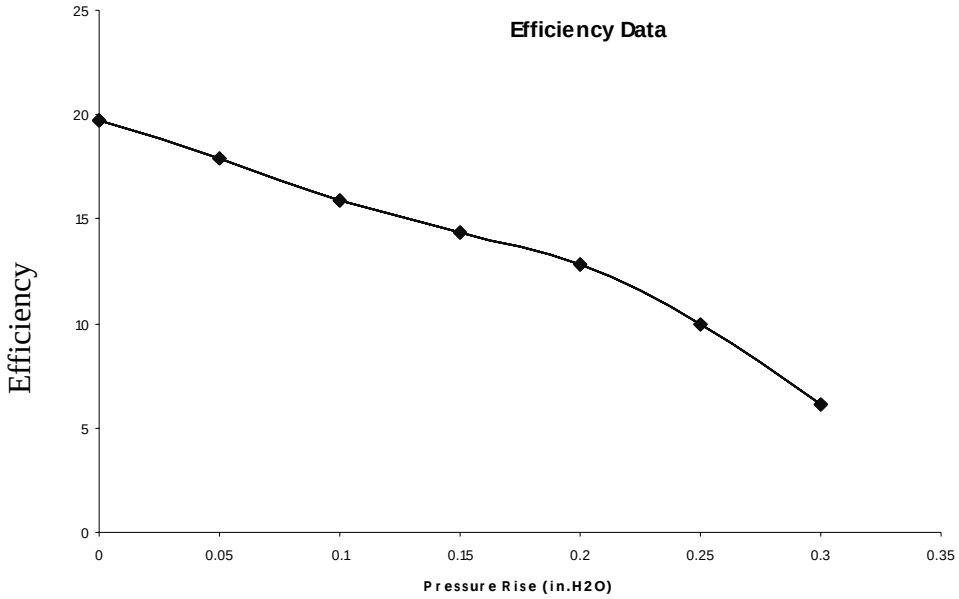

b) fan efficiency (cfm/watt)

Figure 4. Perfrmance dta the aerotech fan assembly of Figure 2.

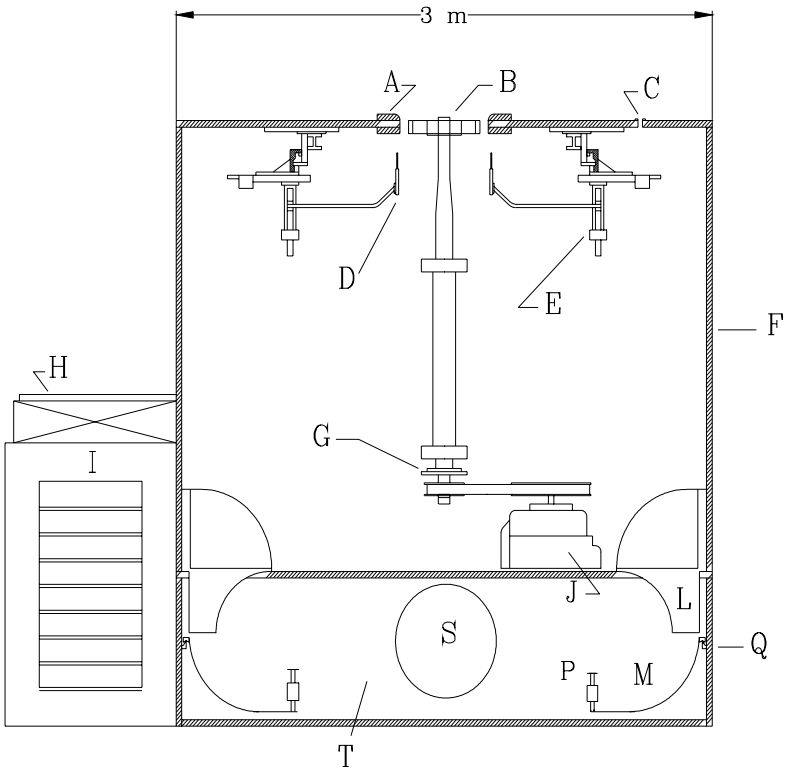

A	AXISYMETRIC SHROUD	J	DRIVE MOTOR
B	TEST FAN	L	NOZZLE
C	PRESSURE TAP	M	TURNING VANE
D	HOT-WIRE PROBE	P	FORCE TRANSDUCER
E	TRAVERSE	Q	TURNING VANE HINGE
F	UPPER RECEIVER	S	INLET TO PRIME MOVER
G	OPTICAL ENCODER	T	LOWER RECEIVER
H	THROTTLE PLATE		
I	PRIME MOVER		

Figure 5. A schematic representation of the aeroshroud. Note, a typical engine mounted fan is shown in this figure. (Drawing is to scale.)

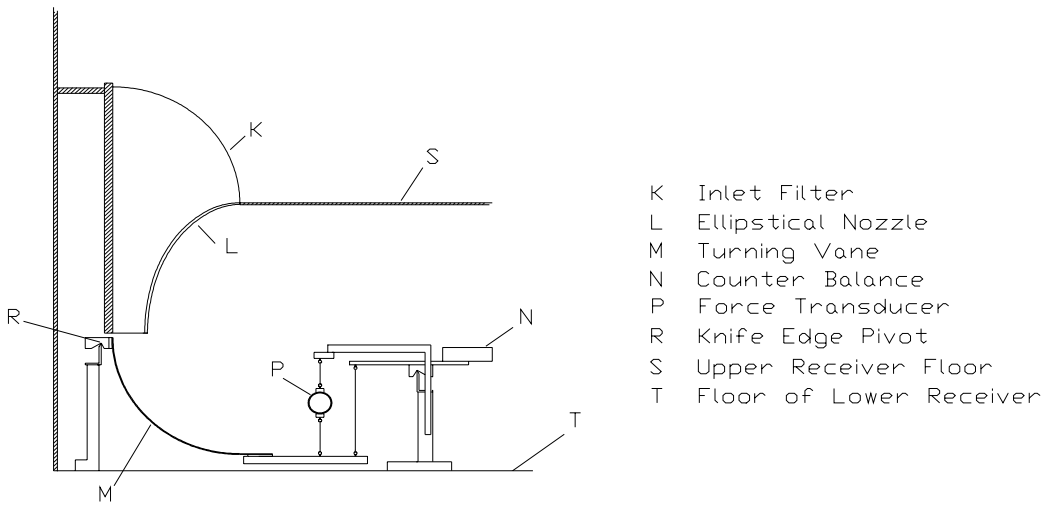

Figure 6. The moment-of-momentum flux device that is used as the flow rate metering techinique in the AFRD.

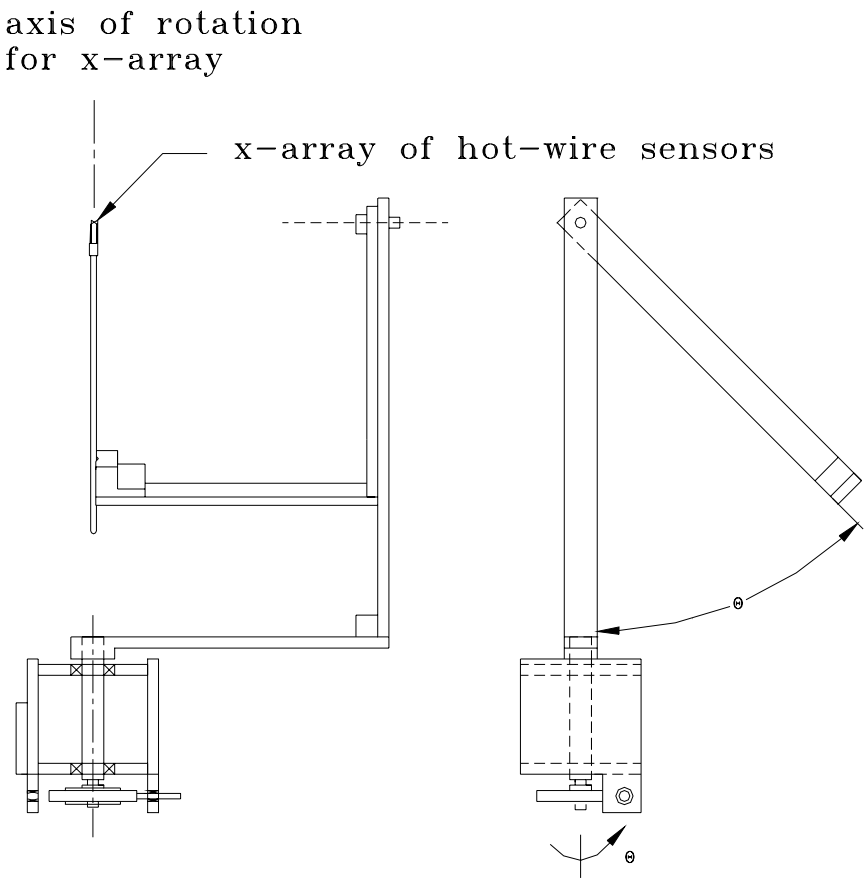

Figure 7. The spherical angle positioning device which allows x-array hot-wire measurements to be aligned with the time mean wake flow at a given r/R position.

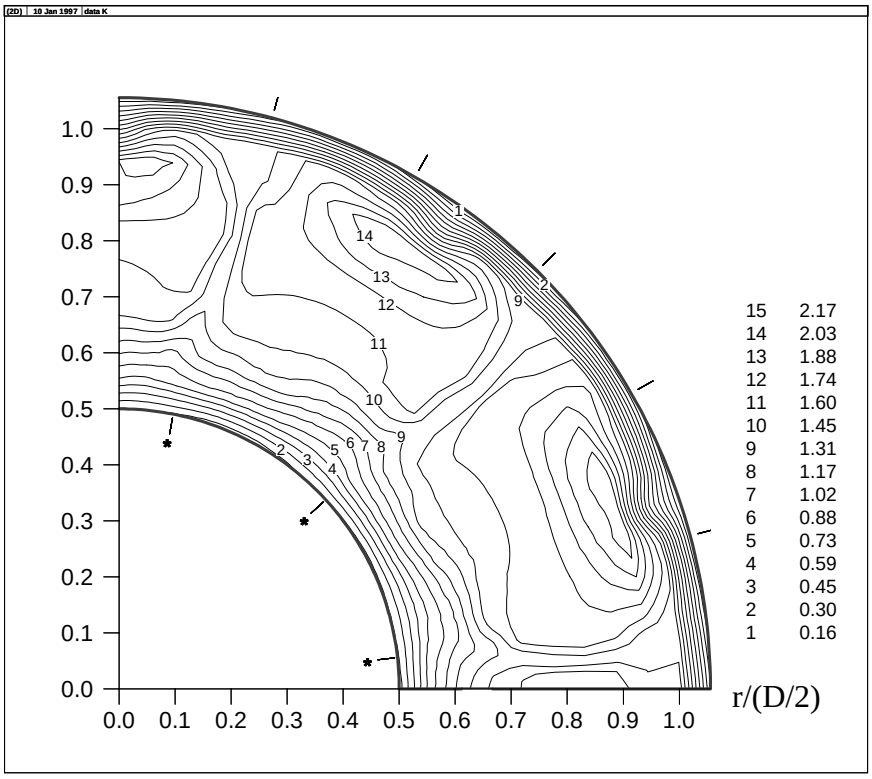

Figure 8. Contours of phase averaged axial velocity: U_x/U_{tip}.
Note: Blade rotation is clockwise.

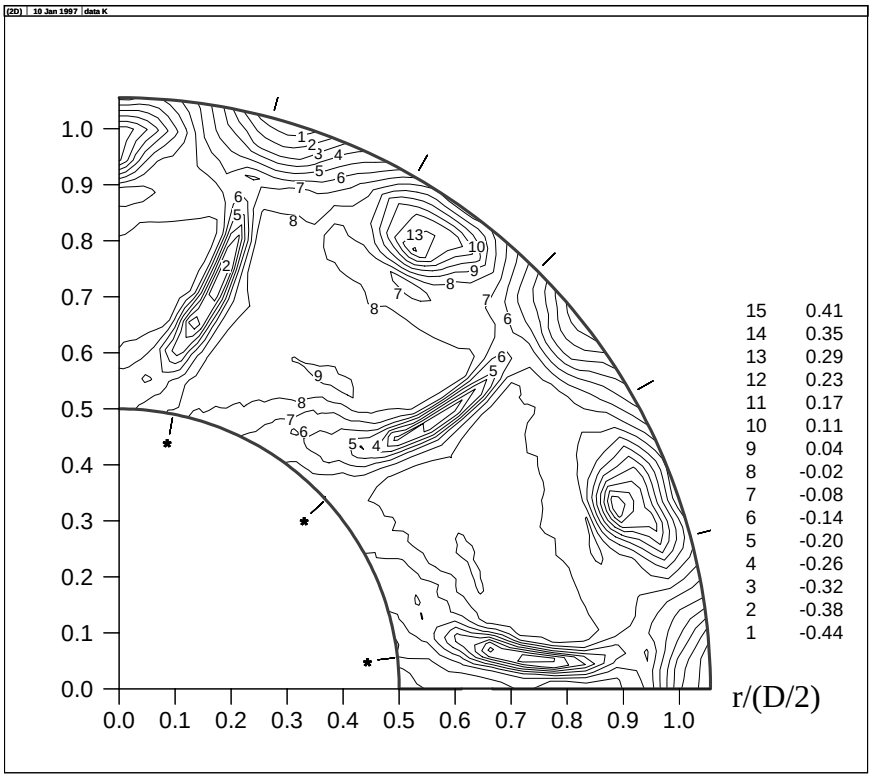

Figure 9. Contours of phase averaged axial vorticity: ω_x/DU_{tip}. Note: Blade rotation is clockwise.

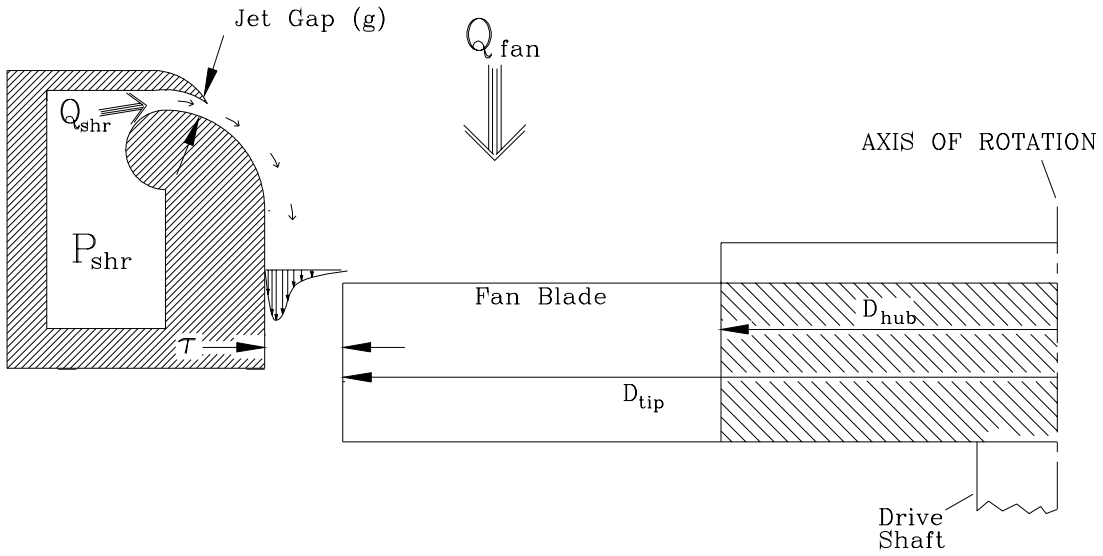

Figure 10. A schematic representation of the aeroshroud. Note, a typical engine mounted fan is shown in this figure.

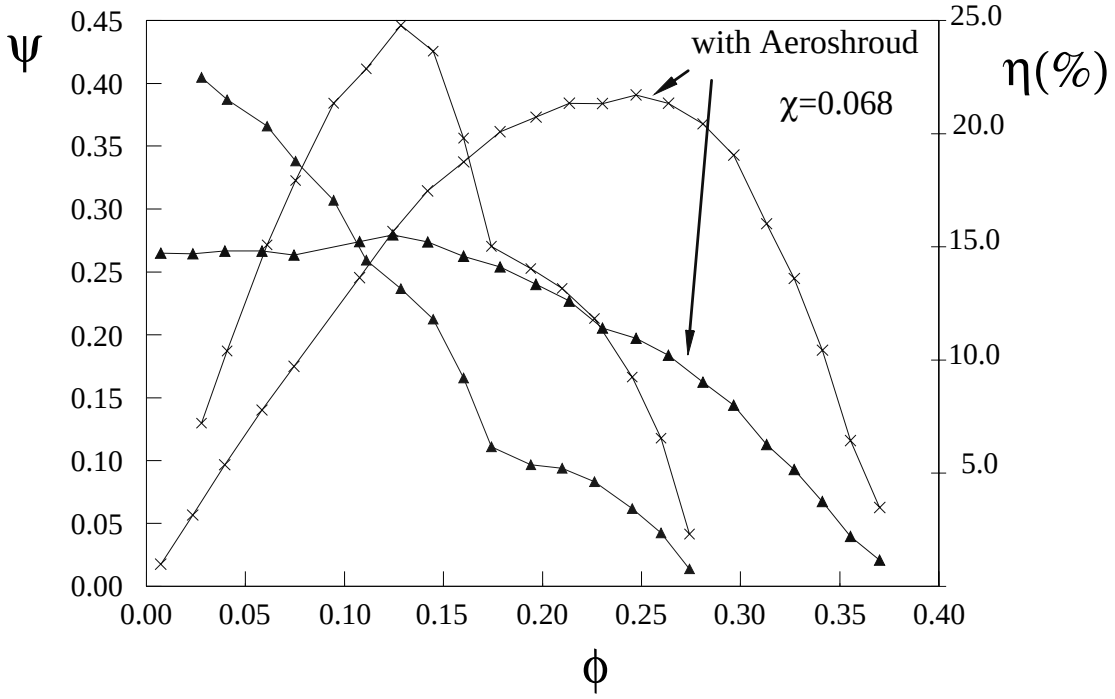

Figure 11. Enhanced cooling fan performance with the aeroshroud of Figure 10. Note, χ is defined in equation 5.

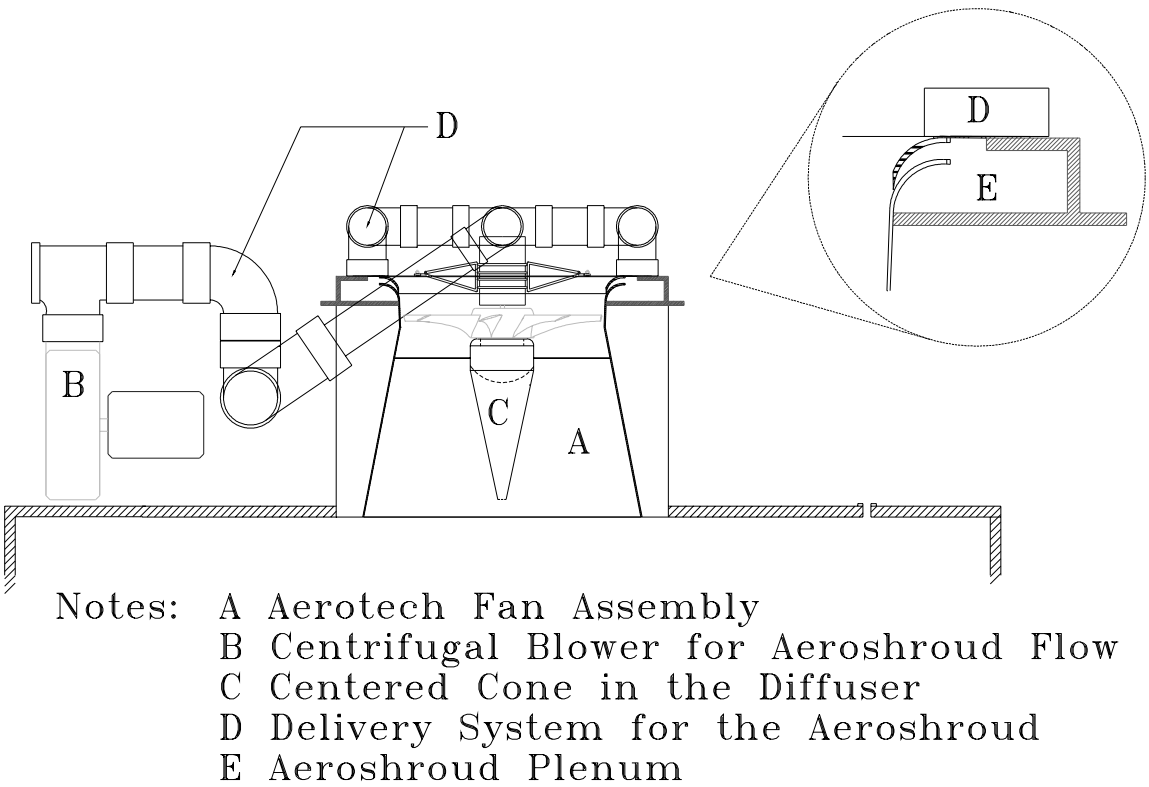

Figure 12. Aeroshroud configuration for the 26 inch fan of Figure 2.